RSC Advances

PAPER

Selective Topotecan Delivery to Cancer Cells by Targeted pH-sensitive Mesoporous Silica Nanoparticles

Received 00th January 20xx,
Accepted 00th January 20xx

DOI: 10.1039/x0xx00000x

www.rsc.org/RSCAdvances

M. Martínez-Carmona,[a,b,c] D. Lozano,[a] M. Colilla[a,b,c,*] and M. Vallet-Regí[a,b,c,*]

Topotecan (TOP), a water-soluble derivative of camptothecin, is a potent antitumor agent that is receiving growing attention for the treatment of several types of cancer. However, one of the major constraints in the clinical use of this drug is its inactivation at the physiological pH of 7.4. Mesoporous silica nanoparticles (MSNs) constitute promising nanocarriers to circumvent this issue. Herein TOP has been encapsulated into MSNs and the nanosystem has been provided of selectivity towards tumor cells, which permits releasing the active form of the molecule at the acidic cell compartments (endo/lysosomes; pH ≤ 5.5) following nanoparticles internalization. For this purpose, MSNs have been coated with a multifunctional gelatin shell that: *i)* protects TOP from hydrolysis and prevents its premature release; *ii)* acts as a pH-sensitive layer; and *iii)* provides multiple anchoring points for the grafting of targeting ligands, such as folic acid (FA), for selective internalization in tumor cells. *In vitro* tests demonstrate that cancer cells, which overexpress membrane cell surface markers with affinity towards FA, internalize higher percentage of nanoparticles than healthy cells, which do not overexpress such markers. Moreover, the nanosystems are efficient at killing tumor cells, whereas they do not decrease viability of normal cells. Contrarily, free TOP failed to kill both cell lines, which can be ascribed to the inactivation of the drug. This novel nanodevice constitutes a step forward toward the design of novel weapons to fight against cancer.

1. Introduction

Topotecan (TOP), a synthetic water-soluble derivative of camptothecin, is a DNA topoisomerase I inhibitor that has gained broad acceptance in clinical use as antineoplastic agent.[1,2] It has been approved by U.S. Food and Drug Administration (FDA) for treating several types of cancer, such as ovarian, cervical and small cell lung.[3] Its antitumor activity is also being investigated, either alone or in combination with other anticancer drugs, in neuroblastoma, Ewing's sarcoma, etc. One of the major limitations of this drug is that under neutral or alkaline conditions, the TOP lactone moiety undergoes a rapid and reversible pH-dependent conversion to a carboxylated open-ring form, which lacks of antitumor activity. On the contrary, in acidic conditions TOP is stable and preserves the active lactone form.[4,5] Thus, clinical trials revealed that the plasma TOP lactone concentration dropped rapidly with a harmonic mean half-life of 3.4 h, being lactone hydrolysis and renal excretion the principal routes of elimination.[6] This requires the administration of high drug doses, which provokes unwanted side-effects in the patient.[7] This issue could be circumvented by using nanocarriers that were selectively internalized by cancer cells and protected TOP from hydrolysis until the active drug was delivered inside the acidic pH of endosomes (pH = 5.5–6.0) or lysosomes (pH = 4.5–5.0).[8] Nonetheless, the selective TOP delivery to cancer cells by targeted pH-responsive nanocarriers still remains a major challenge. Albeit diverse organic[9-14] and inorganic[15-20] nanocarriers have been proposed as TOP nanotherapeutics, none of them have fulfill the above-mentioned conditions. Among inorganic nanocarriers, mesoporous silica nanoparticles (MSNs) own unique properties such as tunable size, shape and porosity, high loading capacity, robustness and easy functionalization, which permit loading diverse antitumor agents.[21,22] Moreover, they exhibit low cytotoxycity[23] and good hemocompatibility,[24] which is mandatory for intravenous administration. All these reasons have made MSNs noteworthy of interest by the scientific community and many targeted stimuli responsive drug delivery systems for antitumor therapy have been reported.[25-37] However, to the best of our knowledge, there are only two pH-responsive TOP MSNs-based systems.[18,19] One of them consists in coordination polymer coated MSNs for the pH-triggered TOP release.[18] The other one involves sophisticated multifunctional enveloped MSNs for subcellular co-delivery of TOP and a therapeutic peptide.[19] Nonetheless, none of them have been designed to be selectively internalized by cancer cells.

[a] *Departamento de Química Inorgánica y Bioinorgánica. Facultad de Farmacia, Universidad Complutense de Madrid. Instituto de Investigación Sanitaria Hospital 12 de Octubre i+12. Plaza Ramón y Cajal s/n, 28040 Madrid, Spain.*
[b] *Centre on Bioengineering, Biomaterials and Nanomedicine (CIBER-BBN), Madrid 28040, Spain.*
[c] *Campus of International Excellence, CEI Campus Moncloa, UCM-UPM, Madrid 28040, Spain.*
** E-mails: vallet@ucm.es; mcolilla@ucm.es*

† Electronic Supplementary Information (ESI) available: Additional characterization, "in vial" and *in vitro* results. See DOI: 10.1039/x0xx00000x

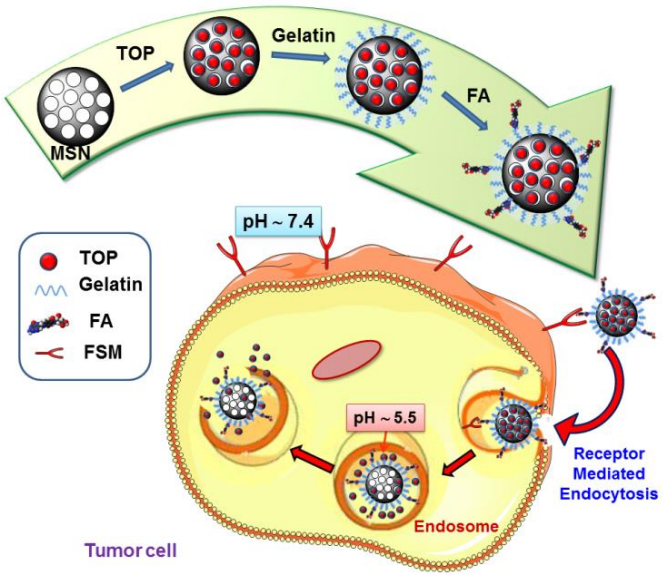

Scheme 1. Schematic illustration of the tumor-targeted TOP nanosystem consisting of MSNs encapsulating TOP, coated with a gelatin shell and decorated with folic acid (FA) as targeting ligand. FSM stands for surface markers with affinity towards FA, which are usually overexpressed in the membrane of certain tumor cells.

Herein we have designed and developed a selective and cost-effective TOP nanodevice able to selectively address cancer cells and once internalized release the active form of the drug in the pH-acidic intracellular compartments (Scheme 1). For this purpose, MCM-41-type MSNs were chosen as TOP nanocarriers. Gelatine coating was chosen as pH-sensitive shell to block the mesopores and prevent premature release, as well as facilitating the grafting of targeting agents. Folic acid (FA) was grafted onto gelatine to provide the system of selective targeting capability to tumour cells, either since its receptor (FA-R)[38-40] or folate binding proteins (FBP)[41] are frequently overexpressed on the surface of human cancer cells. The pH-responsive TOP release performance of the nanosystems was evaluated "in vial", demonstrating that in acidic conditions (pH 5.3) drug release was faster than in physiological conditions of (pH 7.4). Then the capacity of these nanodevices to selectively kill human prostate cancer cells (LNCaP), overexpressing folate binding proteins (FBP), compared to healthy preosteoblast cells (MC3T3-E1), non-overexpressing such membrane proteins, was *in vitro* evaluated. The results indicated the selective internalization of the nanosystems into tumour cells and the efficient pH-dependent TOP release. This novel nanosystem is envisioned as a promising candidate to be incorporated in the existing library of weapons for cancer treatment.

2. Experimental Section

Reactants

The following reagents were purchased from Sigma-Aldrich Inc. (St. Louis, USA): tetraethylorthosilicate (TEOS, 98%), n-cetyltrimethylammonium bromide (CTAB, ≥99 %); sodium hydroxide (NaOH, ≥98 %), ammonium nitrate (NH_4NO_3, ≥98 %), sodium carbonate (Na_2CO_3, ≥99,5 %); fluorescein 5(6)-isothiocyanate (FITC, ≥98 %), (3-aminopropyl)triethoxysilane (APTES, ≥98 %), gelatin Ph Eur, glutaraldehyde grade I 50 wt.% solution in water, folic acid (FA, >97%), N,N'-dicyclohexylcarbodiimide (DCC, 99%), N-hydroxysuccinimide (NHS, 98 %), phosphate-buffered saline (PBS, 10x), hydrochloric acid (HCl, 37%), and topotecan hydrochloride hydrate (TOP, ≥98 %). All other chemicals were purchase in Panreac Química SLU (Castellar del Valles, Barcelona, Spain) inc: absolute ethanol (EtOH), acetone, dimethyl sulfoxide (DMSO), etc., were of the best quality commercially available. All reagents were used as received without further purification. Ultrapure deionized water with resistivity of 18.2 MΩ was obtained using a Millipore Milli-Q plus system (Millipore S.A.S., Molsheim, France).

Characterization Techniques

The powder X-Ray Diffraction (XRD) experiments were performed in a Philips X'Pert diffractometer equipped with Cu Kα radiation (wavelength 1.5406 Å) (Philips Electronics NV, Eindhoven, Netherlands). XRD patterns were collected in the 2θ range between 0.6° and 8° with a step size of 0.02° and counting time of 5 s per step. Thermogravimetric (TG measurements were performed in a Perkin Elmer Pyris Diamond TG/DTA analyser (Perkin Elmer, California, USA), by placing 10 mg of sample in an aluminium crucible and applying 5 ºC/min heating ramps, from room temperature to 600 ºC. Fourier transform infrared spectroscopy (FTIR) was carried out in a Nicolet (Thermo Fisher Scientific) Nexus equipped with a Goldengate attenuated total reflectance device (Thermo Electron Scientific Instruments LLC, Madison, WI USA). Surface morphology was analysed by High Resolution Transmission Electron Microscopy (HRTEM) with a JEOL JEM 3000F instrument operated at 300 kV, equipped with a CCD camera (JEOL Ltd., Tokyo, Japan). Sample preparation was performed by dispersing (aided by an ultrasounds bath) 1 mg of sample in 1 mL of distilled water, and subsequently depositing one drop of the suspension onto carbon-coated copper grids. A solution of 1% of PTA (pH 7.0) was employed as staining agent in order to visualize the organic coating around MSNs.

The hydrodynamic size of nanoparticles by dynamic light scattering (DLS) and zeta (ζ)-potential were measured in a Zetasizer Nano ZS (Malvern Instruments Ltd., United Kingdom) equipped with a 633 nm "red" laser. For this purpose 10 mg of nanoparticles was added to 10 mL of water and the mixture was sonicated for 5 min to get a homogeneous suspension. In the case of ζ-potential measurements the pH was adjusted by adding appropriated amounts of HCl 0.1 M or NaOH 0.1 M to the suspension under magnetic stirring. In both cases, measurements were recorded by placing *ca.* 1 mL of suspension (1mg/mL) in DTS1070 disposable folded capillary cells (Malvern). The textural properties of the materials were determined by N_2 adsorption porosimetry by using a Micromeritics ASAP 2020 (Micromeritics Co., Norcross, USA). To perform the N_2 measurements, *ca.* 30 mg of each sample was previously degassed under vacuum for 24 h at 40 ºC temperature. The surface area (S_{BET}) was determined using the

Brunauer-Emmett-Teller (BET) method and the pore volume (V_P) was estimated from the amount of N_2 adsorbed at a relative pressure around 0.99. The pore size distribution between 0.5 and 40 nm was calculated from the desorption branch of the isotherm by means of the Barrett-Joyner-Halenda (BJH) method. The mesopore size (D_p) was determined from the maximum of the pore size distribution curve.

Synthesis of mesoporous silica nanoparticles (MSN).

Bare MSNs, denoted as MSN, were synthesized by the modified Stöber method using TEOS as silica source in the presence of CTAB as structure directing agent. Thus, 1 g of CTAB, 480 mL of H_2O and 3.5 mL of NaOH (2 M) were added to a 1L round-bottom flask. The mixture was heated to 80 ºC and magnetically stirred at 600 rpm. When the reaction mixture was stabilized at 80 ºC, 5 mL of TEOS were added dropwise at 0.33 mL/min rate. The white suspension obtained was stirred during further 2h at 80 ºC. The reaction mixture was centrifuged and washed three times with water and ethanol. The surfactant was removed by ionic exchange by soaking 1 g of nanoparticles in 500 mL of a NH_4NO_3 solution (10 mg/mL) in ethanol (95%) at 80 ºC overnight under magnetic stirring. MSN were collected by centrifugation, washed three times with ethanol and dried under vacuum at 40 ºC.

Capping of MSN with gelatin (MSNgel)

Capping of MSN with gelatin was performed by adapting a method described elsewhere,[42] affording MSNgel. Thus, 50 mg of MSN were suspended in 5 mL of a gelatin solution (10 mg/mL in PBS 1× pH = 7.4) and left to react for 6 h at 50 ºC. Then, 25 mL of cold PBS 1× (4 ºC) were added. The mixture was gently shaken and then the supernatant was separated by centrifugation and the solid was washed twice with 25 mL of cold PBS. Subsequently, the sample was suspended in 25 mL of fresh cold PBS 1×, 75 μL of a solution of glutaraldehyde (1%), as the crosslinking agent, was added and the mixture was allowed to react overnight in a refrigerator (4 ºC) under magnetic stirring. Crosslinking of gelatin with glutaraldehyde was carried out with the aim of preventing its premature dissolution in aqueous media.[43] Finally, the mixture was centrifuged, washed twice with PBS 1× and dried under vacuum for 24 hours at room temperature.

For cellular internalization and degradation studies fluorescein labeled MSNgel were synthesized. For this purpose, fluorescent gelatin was prepared using a protocol described elsewhere.[44] Briefly, 2.4 g of gelatin and 6 mg FITC was dissolved in 25 mL Na_2CO_3 buffer (pH = 8.5). The solution was heated to 40 ºC under magnetic stirring. After 8 h of reaction in the darkness, the gelatin solution was transferred into a dialysis bag with Mw cutoff of 8000–14,000 Da and immersed in deionized water at 40 ºC to remove the free FITC. The dialysis was performed for 3 days and the water was changed 4–6 times each day. Finally, the solution was poured into a culture dish and dried at 70 ºC to obtain the yellow-colored FITC-modified gelatin slices. Then, the synthesis of fluorescent MSNgel was carried out following the above mentioned methodology for MSNgel but using fluorescent gelatin during the process.

Attachment of Folic Acid to MSNgel (MSN-FA)

10 mg of MSNgel were placed in a vial and suspended in 2 mL of PBS 1× (pH = 7.4). Then, 250 μL of an activated FA solution were added. The activated FA solution was prepared by adding 10 mg of FA and 15 mg of DCC to 250 μL of DMSO at 40ºC. The mixture was stirred for 1h, after that 10 mg of NHS were added and the reaction was allowed to stir for 2 more hours before being added to the MSNgel suspension. The activated FA and MSNgel were kept under magnetic stirring during 5 hours at room temperature. Then, the resulting MSN-FA sample was collected by centrifugation and washed twice with 4 mL of PBS 1× (pH = 7.4) and left to dry under vacuum at 25 ºC. Finally, the synthesis of fluorescent MSN-FA, was carried out following the above mentioned methodology but grafting FA to fluorescein labeled MSNgel.

TOP loading

50 mg of MSN were placed in a dark glass vial and dried at 80ºC overnight under vacuum. Then, 5 mL of an aqueous solution of TOP (3 mg/mL) were added to the vial and the suspension was stirred at room temperature for 48 h. Then, the excess TOP was removed by centrifugation and washed once in water. The amount of drug loaded in MSN was determined from the different between the fluorescence measurements of the initial and the recovered filtrate solutions. Gelatin capping and grafting of FA was then carried out by following the procedures previously described, affording MSN-FA(TOP).

"In vial" TOP release assays

To evaluate the pH-dependent TOP release behaviour of MSN-FA "in vial" release experiments at two different pH values, i.e. 7.4 and 5.3, were performed. For this purpose, two batches of 6 mg of TOP-loaded MSN-FA were prepared. One of them was suspended in 1.5 mL of fresh PBS 10 mM (pH 7.4), and then 0.5 mL of nanoparticles suspension were placed on a Transwell® permeable support with 0.4 μm of polycarbonate membrane (3 replicas were performed). The well was filled with 1.5 mL of PBS 10 mM (pH 7.4) and the suspension was kept under orbital stirring at 100 rpm and 37ºC during all the experiment. The second batch was submitted to the same procedure but using PBS 10 mM (pH 5.3) during the release assay. At every time point studied, the solution outside the Transwell insert was replaced with fresh medium and the amount of TOP released was determined by fluorescence spectrometry (λ_{exc} 400, λ_{em} 530 nm) in a in a BioTek Spectrofluorimeter (BioTek Instruments GmbH, Germany)

In an attempt of elucidating the mechanism that governs the changes induced in the gelatin coating by the variation in the pH (degradation or swelling), two additional experiments were carried out. The first one consisted in suspending fluorescent MSNgel, in PBS at two different pH values (pH 7.4 and pH 5.3)

and kept under magnetic stirring up to 48 h. At given times the medium was replaced by fresh one and the fluorescence of the supernatant was measured. The second one consisted in soaking MSNgel nanosystems into aqueous solutions at the two above mentioned pH values and monitoring the hydrodynamic size of nanoparticles *vs.* time by DLS measurements.

Cell cultures

Cell culture tests were performed using the well-characterized mouse osteoblastic cell line MC3T3-E1 (subclone 4, CRL-2593; ATCC, Mannassas, VA) and androgen-sensitive LNCaP cells, a human prostate cancer cell line (CRL-1740; ATCC, Mannassas, VA). The tested MSNs were placed into each well of 6- or 24-well plates (Corning, CULTEK, Madrid, Spain) after cell seeding. MC3T3-E1 and LNCaP cells were then plated at a density of 30,000 cells cm^2 in 1 mL of α-minimum essential medium or Dulbecco's modified Eagle's medium (DMEM, Sigma Chemical Company), respectively, containing 10% of heat-inactivated foetal bovine serum (FBS, ThermoFisher Scientific, Waltham, MA, USA) and 1% penicillin–streptomycin (BioWhittaker Europe, Verviers, Belgium) at 37 ºC in a humidified atmosphere of 5% CO_2, and incubated for different times. Some wells contained no MSNs as controls.

Cell viability

Cell growth was analysed using the CellTiter 96_ AQueous Assay (Promega, Madison, WI, USA), a colorimetric method for determining the number of living cells in culture. Briefly, both type of cells were cultured as described above without (control) or with the tested materials for several times. At 24 h, 40 µL of CellTiter 96_ AQueous One Solution Reagent (containing 3-(4,5-dimethythizol-2-yl)-5-(3-carboxymethoxy phenyl)-2-(4-sulfophe-nyl)-2H-tetrazolium salt (MTS) and an electron coupling reagent (phenazine ethosulfate) that allows its combination with MTS to form a stable solution) was added to each well and incubated for 4h. The absorbance at 490 nm was then measured in a Unicam UV-500 UV–visible spectrophotometer (Thermo Spectronic, Cambridge, UK).

Confocal laser scanning microscopy (CLSM)

Cellular uptake and internalization of the fluorescence MSNs were observable by CLSM. Cells were incubated with the MSNs (100 µg/mL) for 2 h. Each well was washed with cold PBS for three more times to get rid of the nanoparticles no internalized into the cells, and then fixed with 75% ethanol (kept at −20°C) for 10 min. After being suck the ethanol and washed three times with cold PBS, the nucleus of both types of cells were stained with DAPI for 5 min, respectively, and then washed three times with cold PBS. Cellular uptake of MSNs was recorded by confocal laser scanning microscopy (CLSM) (Leica TCS SP5, Leica Microsystems Co. Ltd., Solms, Germany) with an excitation wavelength at λ = 488 nm. The emission was detected by using a 610-nm long pass filter.

Fluorescence microscopy

Fluorescence microscopy was performed with an Evos FL Cell Imaging System (ThermoFisher Scientific) equipped with tree Led Lights Cubes (lEX (nm); lEM (nm)): DAPY (357/44; 447/60), GFP (470/22; 525/50), RFP (531/40; 593/40) from AMG (Advance Microscopy Group).

Flow cytometry studies

MC3T3-E1 and LNCaP cells were cultured in each well of a 6-well plate. After 24h, the cells were incubated at different times in the absence or presence of the tested MSNs (100 µg/mL). After 2 h, cells were washed twice with PBS and incubated at 37C with trypsin–EDTA solution for cell detachment. The reaction was stopped with culture medium after 5 min and cells were centrifuged at 1.000 rpm for 10 min and resuspended in fresh medium. Then, the surface fluorescence of the cells was quenched with trypan blue (0.4%) to confirm the presence of an intracellular, and therefore internalised, fluorescent signal. Flow cytometry measurements were performed at an excitation wavelength of 488 nm, green fluorescence was measured at 530 nm (FL1). The trigger was set for the green fluorescence channel (FL1). The conditions for the data acquisition and analysis were established using negative and positive controls with the CellQuest Program of Becton–Dickinson and these conditions were maintained during all the experiments. Each experiment was carried out three times and single representative experiments are displayed. For statistical significance, at least 10,000 cells were analysed in each sample in a FACScan machine (Becton, Dickinson and Company, USA) and the mean of the fluorescence emitted by these single cells was used.

3. Results and Discussion

3.1. Characterization of the nanosystems

Mesoporous silica nanoparticles, MSN, were synthetized by a modification of the well-known Stöber method. MSN were coated with gelatine cross-linked with grutaraldehyde, affording MSN-gel and finally folic acid (FA) was grafted to the external surface of MSN-gel, leading to MSN-FA nanosystems. The successful gelatine coating onto MSN and subsequent grafting of FA was confirmed by using different characterization techniques. FTIR spectrum of MSN displays vibration bands in the 490-1090 cm^{-1} range characteristic of pure silica materials (Fig. 1).

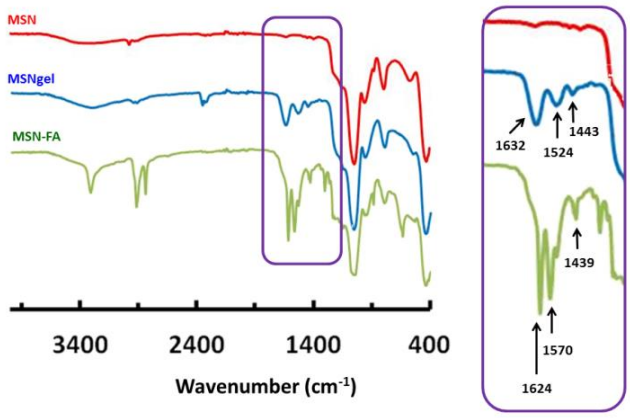

Fig. 1. FTIR spectra of the different nanomaterials synthetized in this work.

FTIR spectrum of MSNgel exhibit additional bands in the 1200-3500 cm^{-1} region, with two main signals centred at 1632 and 1524 cm^{-1} that can be respectively attributed to the C=O and N-H stretching bands of gelatin. The presence of an additional absorption band at *ca.* 1443 cm^{-1}, which can be ascribed to aldimine stretching vibration, would provide further evidence of gelatine crosslinking with glutaraldehyde (Fig. 1). Finally FTIR spectrum of MSN-FA displays signals appearing in the 3600-3000 cm^{-1} range assigned to hydroxyl (-OH) stretching and N-H stretching vibrations bands of FA. A slight displacement of the C=O stretching vibration (1624 cm^{-1}) associated to an increase in the relative intensity of this band would account for a greater the number of amide bonds in this sample due to the reaction between carboxylic acid groups of FA and amine groups of gelatin. Finally, the signal appearing at 1570 cm^{-1} can be assigned to the bending vibration mode of N-H of FA, and the characteristic absorption peak of its phenyl ring appears at 1439 cm^{-1}.

Table 1. Main properties of nanosystems synthetized in this work (N=3).

Material	MSN	MSNgel	MSN-FA
Organic matter (TG) (%)	7.5 ± 0.2	37.2 ± 0.7	58.0 ± 1.2
S_{BET} (m^2/g)	1116 ± 33	27 ± 1	19 ± 1
V_P (cm^3/g)	1.14 ± 0.03	0.14 ± 0.01	0.07 ± 0.01
D_P (nm)	3.0 ± 0.1	-	-
IEP	< 3 ± 0.2	5.3 ± 0.5	4.6 ± 0.4
Mean size (DLS) (nm)	190 ±5	220 ± 25	255 ±14

Table 1 summarizes some of the most relevant features of the nanosystems synthetized in this work. The differences between TG measurements allowed determining the organic matter content incorporated in the nanosystems, being *ca.* 29.7% the amount of gelatin present in MSNgel and *ca.* 20.8% the amount of FA in the final system, MSN-FA.

Low-angle XRD pattern of pristine MSN displays four well resolved peaks that can be indexed as 100, 110, 200 and 210 reflections of a well-ordered 2D-hexagonal structure with *p6mm* space group typical of MCM-41 (Fig. S1). However, XRD patters of MSNgel and MSN-FA only exhibit a weak signal that could be scarcely assigned to 100 reflection. In a first instance, this finding could point to a loss of mesostructural order due to the gelatine coating and FA grafting processes. Nonetheless, it has been widely demonstrated that it is difficult to detect alterations in the crystal structures solely from powder XRD.[45,46] In fact, the disappearance of the signals in XRD patters of coated nanosystems may be also ascribed to the effective filling of the mesopore channels by the gelatin, as it has been previously reported for mesoporous materials functionalized by post-synthesis using great size molecules, such as high generation dendrimers.[47] This would be in agreement with the results derived from N_2 adsorption discussed below, where a decrease in the textural properties of nanosystems takes place due to the incorporation of organic content. Certainly, this affirmation is in agreement with HRTEM studies of the different nanosystems, whose corresponding Fast Fourier Transforms (FT) point to a well order 2D-hexagonal structure, *vide infra*.

N_2 adsorption-desorption isotherms are of type IV corresponding to mesoporous materials (Fig. S2). The appropriate treatment of the experimental data evidence the decrease in the textural parameters of samples once coated by gelatine and gelatine-FA, which allowed confirming the efficiency of the coating process. The decrease in the surface area (S_{BET}) from 1116 m^2/g for MSN to 27 m^2/g and 19 m^2/g for MSNgel and MSN-FA, respectively. The exceptional decrease in surface area accessible to N_2 in the gelatine-containing samples accounts for the successful coating of the MSN core, in agreement with TEM, vide infra. The pore volumes (V_P) also experience a dramatically decrease, dropping from 1.14 cm^3/g for MSN to 0.14 cm^3/g and 0.07 cm^3/g for MSNgel and MSN-FA, respectively. The union of folic acid to gelatin (MSN-FA) produces a slight decrease in the surface area and pore volume still available in MSNgel. This may be ascribed to the large amount of FA anchored to the gelatin shell (*ca.* 20% according to TGA). Thus FA itself could be blocking some of the remaining porosity accessible to N_2. Another fact to take into account is that the FA grafting is carried out in the presence of DCC and NHS. As it has been reported in the literature this mixture acts as gelatin cross-linker,[48] which would explain a higher biopolymer crosslinking degree and therefore would lead to a decrease in the textural properties (S_{BET} and V_P) of the resulting nanosystem.

Pore diameter (D_P) was *ca.* 3.0 nm for MSN whereas it could not be determined in the case of MSNgel and MSN-FA samples. All these findings may account not only to the external covering of MSN by organic coatings but also the partial occupation of the mesoporous cavities organic matter, in agreement with XRD results.

TEM images and their corresponding FT of samples confirm a honeycomb mesoporous arrangement typical of MCM-41 (Fig. 2). The coating and FA grafting processes do not affect the mesostructural order of MSN. The morphology of the nanoparticles is neither influenced, showing spherical particles in all cases. Staining of samples with phosphotungstic acid (PTA) allowed observing the organic coatings as high contrast areas and the inorganic silica matrix as brighter zones in TEM images. The average diameter of the nanosystems estimated

from the 20 measurements was *ca.* 170 nm, 180 nm and 190 nm for MSN, MSNgel and MSN-FA, respectively. Moreover, the average thickness of the organic shell determined from 20 measurements was *ca.* 4 nm and 6 nm for MSNgel and MSN-FA, respectively.

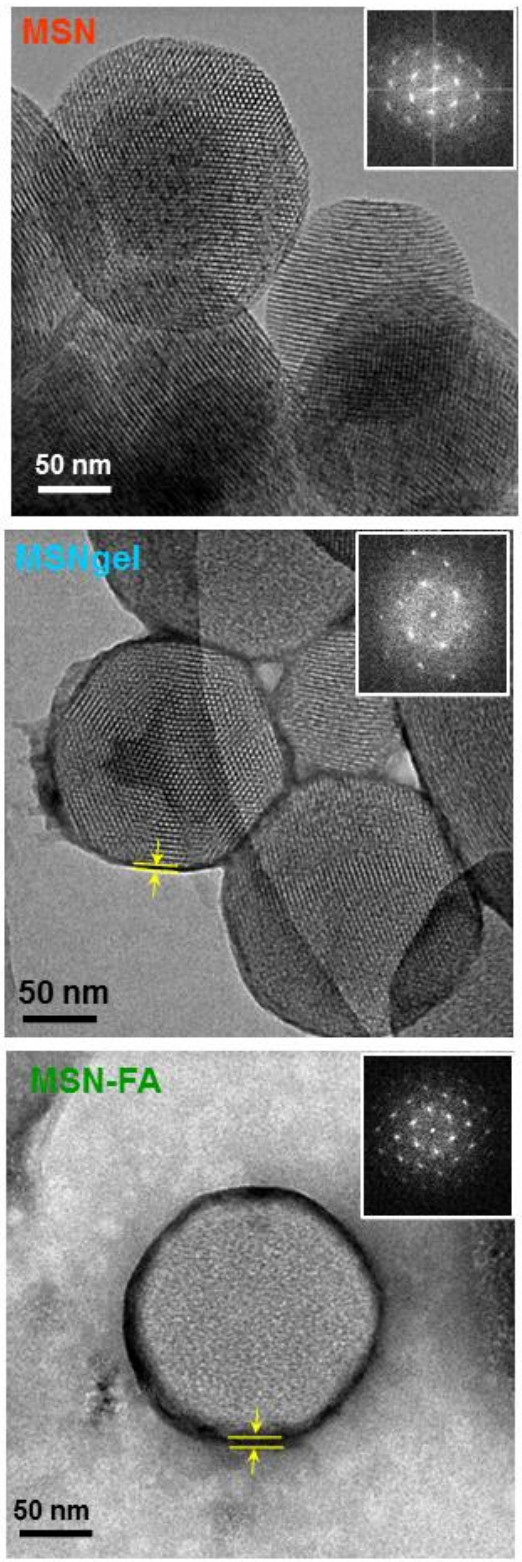

Fig. 2. TEM images and their corresponding FT of the different nanosystems synthetized in this work. Samples were stained with 1% of phosphotungstic acid (PTA).

To get information about the hydrodynamic size and surface charge of the nanosystems, dynamic light scattering (DLS) and ζ-potential measurements were recorded in suspensions of these materials in water. The mean sizes determined by DLS in water were found to be 190 nm, 220 nm and 255 nm for MSN, MSNgel and MSN-FA samples, respectively (Fig. S3), which reasonably were slightly higher than those estimated from TEM images. This fact can be explained because DLS provides the hydrated hydrodynamic diameter whereas TEM shows the size in a dry state.[49] As expected, these differences are more pronounced in MSNgel and MSN-FA because the presence of the hydrophilic polymeric coatings allows the formation of thicker hydration layers than in MSN.[50]

The isoelectric point (IEP) of samples, which is tightly related with the zero-surface charge value (ζ-potential = 0) of these particles (Table 1) were estimated by recording ζ-potential *vs* pH plots (Fig. S4). The different profiles of the plots and IEP account for the successfully coating with gelatin and FA grafting.

3.2. "In vial" pH-responsive TOP release performance

TOP was loaded into MSN by soaking suspensions of 50 mg nanoparticles in 5 mL of a concentrated solution of TOP (3 mg/mL) (for further details see Experimental Section). The amount of TOP loaded into MSN was found to be *ca.* 5% in weight. The successful drug loading was confirmed by the decrease in the V_P measured by N_2 adsorption (data not shown).

With the aim of evaluating the performance of the complete nanosystem, MSN-FA, under physiological relevant conditions mimicking extracellular conditions (pH = 7.4) and those of endosomes or lysosomes (pH ≤ 5.5) TOP release assays were carried out "in vial". Fig. 3 shows the TOP release profiles from MSN-FA after soaking the nanosystem into aqueous solutions at pH 7.4 and pH 5.3 during 48 hours. Release profiles can be adjusted to first-order kinetic model by introducing an empirical non-ideality factor (δ) to give the equation:[51]

$$Y = A(1 - e^{-kt})^{\delta} \qquad \text{(Eq. 1)}$$

with Y being the percentage of TOP released at time *t*, *A* the maximum amount of TOP released (in percentage), and *k*, the release rate constant. In this approach, the values for δ are comprised between 1 for materials that obeys fist-order kinetics, and 0, for materials that release the loaded drug in the very initial time of test. The parameters of the kinetic fitting shown in Fig. 3 and Table S1, indicate that TOP release is faster at pH 5.3 than at pH 7.4. In this case the value of δ is very similar, *ca.* 0.5, in both cases, but higher amount of TOP is release upon acidification of the medium compared to the amount released without acidic stimulus.

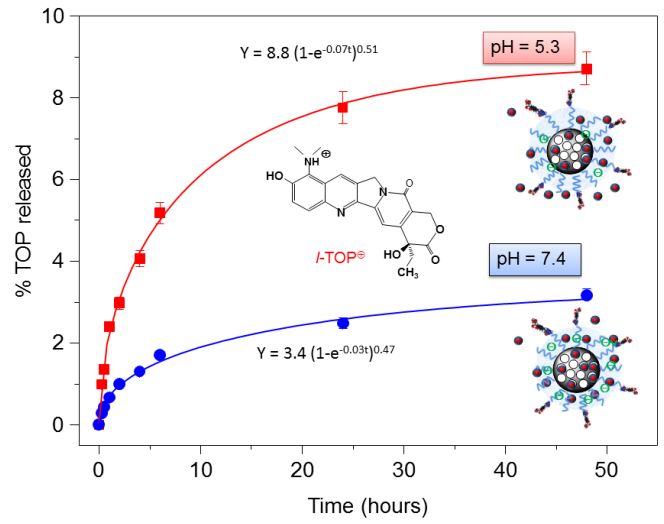

Fig. 3. "In vial" cumulative TOP release (in percentage) *vs* time from MSN-FA nanosystems when soaked in phosphate buffer solution (PBS) at pH 5.3 and pH 7.4 for 2 days.

Different hypotheses may be postulated to explain this pH-responsive drug release behaviour (Fig. S5). The first one relies on the degradation of the gelatin in the "in vial" acidic conditions. For this purpose, as described in the Materials and Methods Section, fluorescent MSNgel, were synthesized. Suspensions of fluorescent MSNgel were prepared in PBS at the two different pH values of pH 7.4 and pH 5.3 and fluorescence of the medium at given time periods was measured. The absence of fluorescence signal due to fluorescein in both experiments accounts for the lack of degradability of the gelatin coating. This is in agreement with previous results found in the literature for crosslinked-gelatine, which does not undergo any appreciable degradation in aqueous solution.[52]

The second hypothesis postulates that when the core-shell MSN-gelatin nanosystems are soaked in aqueous media the functional groups of gelatin change their ionization state, which originates a process of electrostatic repulsions that provokes pH-dependent gelatin swelling. It is well-known that when polymeric chains have ionisable groups there are electrostatic repulsion between such groups, which increases the volume of the polymeric chains and also the swelling capacity of the polymer coating. The main composition of gelatin is polypeptides containing carbonyl, amino and amide functional groups that opens the possibility to be positively or negatively charged depending on the pH.[42,53] Therefore, the gelatine structure is ionisable because of these equilibria:[54]

$$-NH_2 + H_2O \leftrightarrow -NH_3^+ + OH^- \quad pK_b \sim 6.5 \qquad \text{(Eq. 2)}$$

$$-COOH + H_2O \leftrightarrow -COO^- + H_3O^+ \quad pK_a \sim 4.7 \qquad \text{(Eq. 3)}$$

In acid medium the present chemical species of the gelatin are NH_3^+ and COOH; in basic medium the predominant species are NH_2 and COO^-; and in pH's between 4.0 and 7.0 the existing species are anyone of the above-mentioned functional groups, *i.e.*, NH_3^+, COO^-, NH_2 or COOH. Thus, in acidic medium, the swelling is controlled mainly by the repulsion between NH_3^+ groups, in basic medium by $-COO^-$, and between pH 4.0 and 7.0 by NH_3^+ and COO^-. In an attempt to investigate the differences in the gelatin swelling degree between pH 5.3 and 7.4, MSNgel suspensions into aqueous solutions at these two pH values were prepared and the hydrodynamic size of nanoparticles by DLS *vs.* time was recorded. However, no differences in the MSNgel diameters were appreciated. This could be ascribed to the swelling degree of MSNgel at both pH, which could not be detected by DLS due to the broad nanoparticles size distributions (Fig. S3).

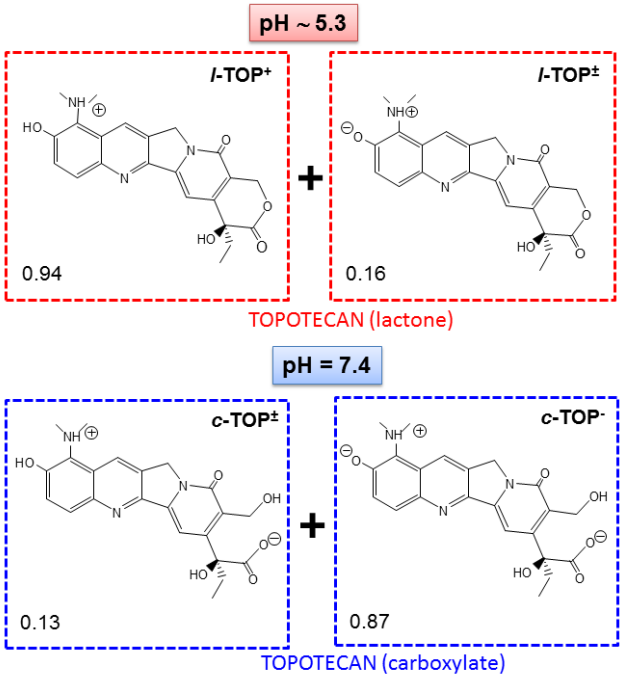

Fig. 4. TOP species and their relative abundance at pH 5.3 (top) and at pH 7.4 (bottom).

Finally, the host/guest MSN-FA/TOP interactions cannot be overruled, since they are the driving forces that govern kinetic release profiles from hybrid mesoporous materials.[55] As previously mentioned, it is well-known that the confinement of sensitive drugs into mesoporous cavities and appropriate pore capping is a widely exploited strategy to avoid cargoes degradation. Thus, taking into account that the most abundant specie of TOP in its active form is the cationic lactone *I*-TOP^+ (Fig. 4), and knowing that MSN are negatively charged due to the silica walls (Fig. S4) the next step was to investigate the variations in the surface charge of MSN-FA *vs* pH. This may govern the interaction with the *I*-TOP^+ during its diffusion out of the nanosystem. ζ-potential values of MSN-FA at pH 5.3 and pH 7.4 are respectively *ca.* -14 and -26 mV, respectively. In both cases the negatively charged surface of silica walls may interact with the positively charged drug, being responsible of slowing down the TOP release from the nanosystems at both pH values. However, once the drug diffuses out of the silica network it has to pass across the gelatin barrier. Thus,

positively charged drug remains more retained in MSN-FA at pH 7.4 than at pH 5.3 because of the greater electrostatic attractive interactions with the net negative charge of the former. This would really explain the different release profiles found for TOP from MSN-FA at the two different pH values.

For comparative purposes, "in vial" TOP delivery assays where carried out from pure-silica MSN at pH 5.3 and pH 7.4 (Fig. 5). In this case there is not a protecting barrier that impedes the diffusion of the delivery medium inside the mesopores. Thus, at pH 5.3 94% of drug is expected to be in the lactone cationic form *l*-TOP$^+$, and at pH 7.4 87% of TOP would be in the anionic hydrolyzed carboxylate *c*-TOP- and 15% as zwitterionic *c*-TOP$^\pm$ (Fig. 4). Fig. S6 demonstrates that, independently of the pH, TOP release in MSN is faster than in MSN-FA, since there is not capping layer that slow down the departure of the drug in the former. Indeed, contrarily to that occurring in MSN-FA, in this case, TOP release from MSN is faster at pH 7.4 than at pH 5.3 (see Table S1 for the parameters of the kinetic fitting). Thus, after 48 of assay 78% and 35% of drug is released from MSN at pH 7.4 and pH 5.3, respectively. At both pH values, ζ-potential measurements indicate a similar surface charge for MSN of around -30 mV (Fig. S4), but the TOP predominant species varies. TOP is hydrolyzed to *c*-TOP$^-$ at pH 7.4 results in a weaker drug to MSN interaction, hence very fast release is achieved. On the contrary, at pH 5.3 TOP preserves its active cationic lactone form *l*-TOP$^+$ capable to undergo electrostatic attractive interactions with the negatively charged MSN silica walls.

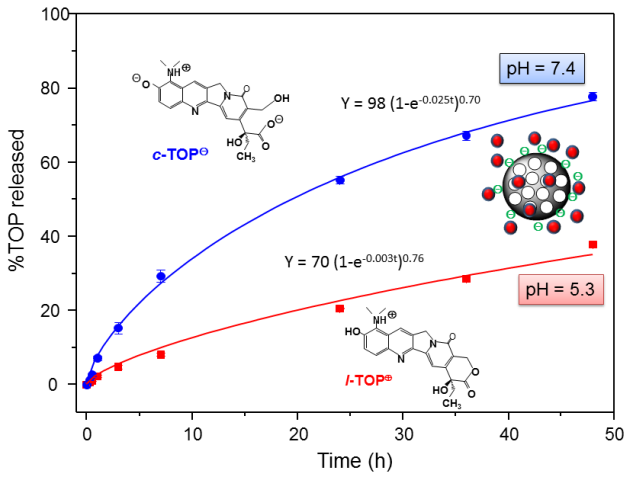

Fig. 5. "In vial" cumulative TOP release profiles (in percentage) *versus* time from MSN nanosystems when soaked in phosphate buffer solution (PBS) at pH 5.3 and pH 7.4 for 2 days.

3.3. *In vitro* behaviour of the nanosystems

Once MSN-FA nanosystem was fully characterized and its pH-sensitive TOP release capability was evaluated "in vial", the next step was to study its *in vitro* behaviour as selective carrier for targeted TOP delivery. For this purpose, we cultured MSNgel and MSN-FA nanosystems in presence of two types of cells populations: MC3T3-E1 and LNCaP cells. LNCaP is a human prostate cancer cell line that overexpresses folate binding proteins (FBP), with high affinity towards FA,[41] and MC3T3-E1 is a preosteoblastic cell line that, as normal cell, minimally expresses membrane surface markers with affinity towards FA.[56,57]

The *in vitro* cytotoxicity study was determined by the exposition of MC3T3-E1 and LNCaP cells to different amounts of nanoparticles (20, 50 and 100 µg/mL). It was observed that none of the studied materials, neither MSNgel (Fig. 6a) nor MSN-FA (data not shown), induced significant cytotoxicity measured by a MTS assay (cell viability was in all cases > 99% that of the control) or affected to the morphology in both type of cells, as observed by fluorescence microscopy (Fig. S6).

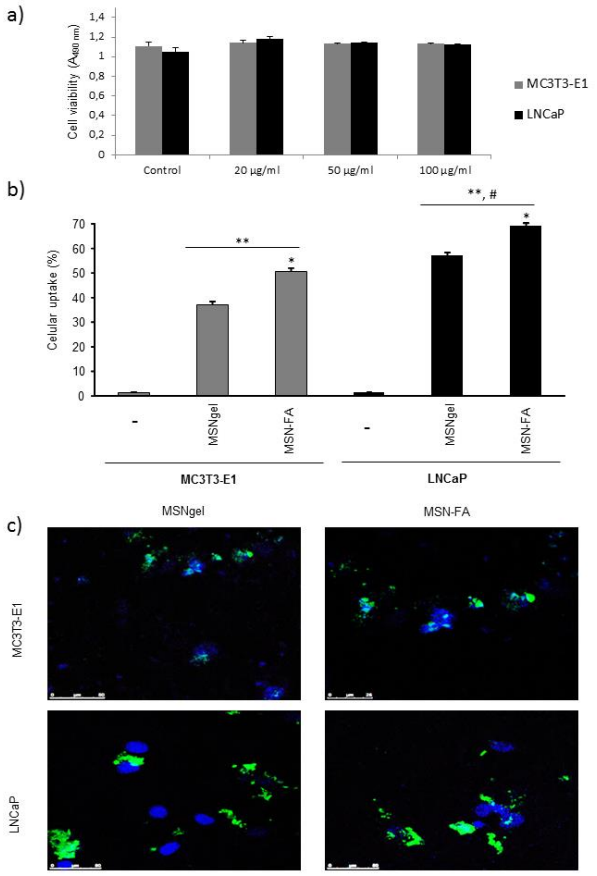

Fig. 6. (a) Cell viability in contact with different concentrations of nanoparticles. Similar proliferation results were obtained in contact with MSN-FA. (b) Cellular uptake in the presence of MSNgel and MSN-FA at 2 hours, measured by flow cytometry. (c) Fluorescence confocal laser scanning microscopy images of MC3T3-E1 and LNCaP cells incubated with MSNgel and MSN-FA at 2 hours of cell culture. *p<0.05 *vs* corresponding MSNgel control; **p<0.05 *vs.* corresponding control without nanoparticles #p<0.05 *vs.* corresponding control and same condition in MC3T3-E1 cells (Student´s t-test).

Cellular uptake and internalization of the nanosystems were observable by flow cytometry and confocal microscopy in MC3T3-E1 and LNCaP cells in contact with the different nanoparticles (100 µg/mL) for 2 hours (Fig. 6b). After 2 hours, MSN-FA internalization in LNCaP increases and it is always higher compared with the internalization degree within MC3T1-E1 preosteoblastic cells. However slightly internalization of MSN-FA is also observed in MC3T3-E1

because these cells also exhibit folate surface markers at the cell membrane, although are not overexpressed. Flow cytometry results give away that MSN-FA are internalized through a FBP mediated mechanism within tumour cell line LNCaP.

The cellular uptake results obtained by flow cytometry were also confirmed by confocal microscopy using fluorescein labeled nanoparticles (Fig. 6c). No fluorescence was observed in the end slices corresponding to the external cellular surfaces, suggesting that the nanoparticles did not adsorb on the cell membranes. Therefore, the modifications presents in the MSN-FA nanoparticles (100 µg/mL) improve the cellular uptake (in a very short time, 60 min) compared to MSNgel in both type of cells but especially in LNCaP cells. These results are in concordance with the overexpression of FBP in these tumor cells and the higher affinity by MSN-FA nanoparticles. This higher affinity for cancer cells overexpressing FBP made MSN-FA promising drug nanocarriers to be targeted to this type of tumour cells.

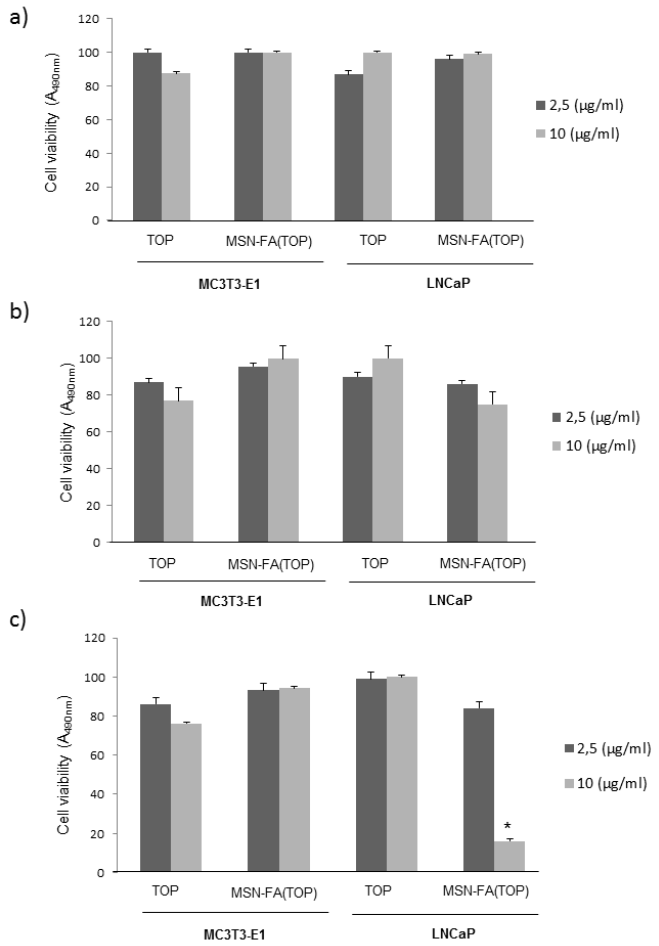

Fig. 7. Cell viability in contact with different concentrations of TOP (2.5 and 10 µg/mL) loaded or not into MSN-FA at a) 24, b) 48 and c) 72 hours of cell culture. *p<0.05 *vs* TOP not loaded into MSN-FA (Student´s t-test).

In addition, we performed an *in vitro* cytotoxicity study with TOP concentrations (2.5 and 10 µg/mL) loaded or not in MSN-FA nanoparticles in presence of MC3T3-E1 or LNCaP cells at different times (24, 48 and 72h, Fig. 7 a-c). It was observed that any concentration of TOP, loaded or not in MSN-FA nanoparticles, induced significant cytotoxicity at 24 or 48 hours (Fig. 7 a,b). Furthermore, TOP loaded or not in MSN-FA failed to affect MC3T3-E1 cell viability too at 72h and only TOP (10 µg/mL) loaded in MSN-FA nanoparticles significantly decreased the cell viability in tumour LNCaP cells at this time (Fig. 7c). These findings suggest that the decrease in LNCaP viability at 72h, and not before, can be due to the slow release of TOP loaded into the MSN-FA nanoparticles that was previously demonstrated (Fig. 3). On the other hand, we observed this effect only in LNCaP cells because, as previously commented, LNCaP overexpresses FBP with high affinity towards FA, and MC3T3-E1 does not. In addition, these results are in concordance with the observed higher internalization degree of MSN-FA nanoparticles in LNCaP cells (Fig. 6b).

3. Conclusions

In conclusion, an innovative nanosystem able to selectively deliver TOP to tumor cells has been developed. MSNs has been employed as nanocarriers and a gelatin shell has been used as multifunctional coating able to prevent TOP departure and therefore protecting it from inactivation by hydrolysis at the physiological pH of 7.4, which constitutes one of the major issues in the clinical application of this drug. In addition, biopolymer coating governs pH-dependent TOP kinetics and provides multiple anchorage points for the grafting of targeting ligands, which promote selectivity towards cancer cells overexpressing surface markers with affinity towards such ligands. *In vitro* assays demonstrated that these targeted nanosystems selectively killed tumor cells, whereas free TOP failed to affect viability of both tumor and cell lines. This novel nanosystem constitutes a significant advance towards the development of a library of nanomedicines for antitumor therapy.

Acknowledgements

This work was financially supported by Ministerio de Economía y Competitividad (MINECO), Spain, through projects MAT2012-35556, MAT2015-64831-R and CSO2010-11384-E (Agening Network of Excellence). M. Martínez-Carmona also thanks Moncloa Campus of International Excellence (UCM-UPM) for a PICATA predoctoral fellowship. D.L. is recipient of postdoctoral research contract from MINECO (FPDI-2013–17268). We also thank the X-ray Diffraction C.A.I. and the National Electron Microscopy Centre, UCM.

Notes and references

1 Y. H. Hsiang, R. Hertzberg, S. Hecht and L. F. Liu, *J Biol Chem.*, 1985, **25**, 14873.

2 P. D'Arpa and L. F. Liu, *Biochim. Biophysica Acta,* 1989, **989**, 163.

3 J. F. Pizzolato and L. B. Saltz, *Lancet,* 2003, **361**, 2235.
4 V. M. Herben, W. W. ten Bokkel Huinink and J. H. Beijnen, *Clin. Pharmacokinet,* 1996**, 31**, 85.
5 P. Tardi, E. Choice, D. Masin, T. Redelmeier, M. Bally and T. D. Madden, *Cancer Res.,* 2000, **60**, 3389.
6 J. G. Wall, H. A. 3rd Burris, D. D. Von Hoff, G. Rodriguez, R. Kneuper-Hall, D. Shaffer, T. O'Rourke, T. Brown, G. Weiss, G. Clark, S. J. B. McVea, R. Johnson, C. Friedman, B. Smith, W. S. Mann and J. Kuhn, *Anti-Cancer Drug,* 1992, **3**, 337.
7 B. Arun and E. P. Frenkel, *Expert Opin. Pharmacother.,* 2001, **2**, 491.
8 R. J. Gillies, N. Raghunand, M. L. García-Martín and R. A. Gatenby, *IEEE Eng. Med. Biol. Mag.*, 2004, **23**, 57.
9 Y. –L. Hao, Y. –L. Deng, Y. Chen, A. –J. Hao, Y. Zhang and K. –Z. Wang, *J. Pharm. Pharmacol*., 2005, **57**, 1279.
10 N. A. Patankar, D. Waterhouse, D. Strutt, M. Anantha and M. B. Bally, *Invest. New Drug.,* 2013, **31**, 46.
11 D. C. Drummond, C. O. Noble, Z. Guo, M. E. Hayes, C. Connolly-Ingram, B. S. Gabriel, B. Hann, B. Liu, J. W. Park, K. Hong, C. C. Benz, J. D. Marks and D. B. Kirpotin, *J. Control. Release,* 2010, **141**, 13.
12 K. D. Fugit and B. D. Anderson, *J. Control. Release,* 2014, **174**, 88.
13 L. G. Souza, E. J. Silva, A. L. L. Martins, M. F. Mota, R. C. Braga, E. M. Lima, M. C. Valadares, S. F. Taveira and R. N. Marreto, *Eur. J. Pharm. Biopharm.,* 2011, **79**, 189.
14 S. Padhi, M. Mirza, D. Verma, T. Khuroo, A. K. Panda, S. Talegaonkar, R. K. Khar and Z. Iqbal, *Drug Deliv.* 2015, 1.
15 M. Kim, K. Ock, K. Cho, S. –W. Joo and S. Y. Lee, *Chem. Commun.,* 2012, **48**, 4205.
16 M. R. di Nunzio, V. Agostoni, B. Cohen, R. Gref and A. Douhal, *J. Med. Chem.*, 2014, **57**, 411.
17 X. Du, B. Shi, J. Liang, J. Bi, S. Dai and S. Z. Qiao, *Adv. Mater.,* 2013, **25**, 5981.
18 L. Xing, H. Zheng, Y. Cao and S. Che, Adv. Mater., 2012, **24**, 6433.
19 G. –F. Luo, W. –H. Chen, Y. Liu, Q. Lei, R. –X. Zhuo and X. –Z. Zhang, *Sci. Reports,* 2014, **4**, article number: 6064.
20 B. Shen, K. Zhao, S. Ma, D. Yuan and Y. Bai, *Chem. Asian. J*., 2015, **10**, 344.
21 M. Vallet-Regí, A. Rámila, R. P. del Real and J. Pérez-Pariente, *Chem. Mater.,* 2001, **13**, 308.
22 M. Vallet-Regí, F. Balas and D. Arcos, *Angew. Chem. Int. Ed.,* 2007, **46**, 7548.
23 J. Lu, M. Liong, Z. X. Li, J. I. Zink and F. Tamanoi, *Small,* 2010, **6**, 1794.
24 Y. Zhao, X. Sun, G. Zhang, B. G. Trewyn, I. I. Slowing and V. S. Lin, *ACS Nano,* 2011, **5**, 1366.
25 P. Yang, S. Gai and J. Lin, *Chem. Soc. Rev.,* 2012, **41**, 3679.
26 C. Argyo, V. Weiss, C. Braeuchle and T. Bein, *Chem. Mater.,* 2014, **26**, 435.
27 E. Aznar, M. Oroval, L. Pascual, J. R. Murguía, R. Martínez-Máñez and F. Sancenón, *Chem. Rev.,* 2016, **116**, 534.
28 F. Tang, L. Li and D. Chen, *Adv. Mater*., 2012, **24**, 1504.
29 Z. Li, J. C. Barnes, A. Bosoy, J. F. Stoddart and J. I. Zink, *Chem. Soc. Rev.,* 2012, **41**, 2590.
30 A. Baeza, E. Guisasola, A. Torres-Pardo, J. M. González-Calbet, G. J. Melen, M. Ramírez and M. Vallet-Regí. *Adv. Funct. Mater*., 2014, **24**, 4625.
31 Y. Zhang, C. Y. Ang, M. Li, Y. Tan, Q. Qu, Z. Luo and Y. Zhao, *ACS Appl. Mater. Interfaces,* 2015, **7**, 18179.
32 J. L. Paris, M. V. Cabañas, M. Manzano and M. Vallet-Regí, *ACS Nano,* 2015, **9**, 11023.
33 M. Martínez-Carmona, A. Baeza, M. A. Rodríguez-Milla, J. García-Castro and Vallet-Regí, *J. Mater. Chem. B*, 2015, **3**, 5746.
34 G. Villaverde, A. Baeza, G. J. Melen, A. Alfranca, M. Ramírez and M. Vallet-Regí, *J. Mater. Chem. B,* 2015, **3**, 4831.
35 M. R. Villegas, A. Baeza, M. Vallet-Regí, *ACS Appl. Mater. Interfaces,* 2015, **7**, 24075.
36 M. Martínez-Carmona, M. Colilla and M. Vallet-Regí, *Nanomaterials,* 2015, **5**, 1906.
37 A. Baeza, M. Manzano, M. Colilla and M. Vallet-Regí, *Biomater. Sci.,* 2016, **4**, 803.
38 W. A. Franklin, M. Waintrub, D. Edwards, K. Christensen, P. Prendegrast, J. Woods, P. A. Bunn and J. F. Kolhouse, *Int. J. Cancer.,* 1994**, 8**, 89.
39 S. D. Weitman, R. H. Lark, L. R. Coney, D. W. Fort, V. Frasca, V. R. Jr. Zurawski and B. A. Kamen, *Cancer Res.,* 1992, **52**, 3396.
40 J. Lu, Z. Li, J. I. Zink and F. Tamanoi, *Nanomed. Nanotechnol. Biol. Med.,* 2012, **8**, 212.
41 Y. Hattori and Y. Maitani, *J. Control. Release,* 2004, **97**, 173.
42 Z. Zou, D. He, X. He, K. Wang, X. Yang, Z. Qing and Q. Zhou, *Langmuir,* 2013, **29**, 12804.
43 Y. Tabata and Y. Ikada, *Adv. Drug Deliver. Rev.,* 1998, **31**, 287.
44 Z. Cheng, Y. Dai, X. Kang, C. Li, S. Huang, H. Lian, Z. Hou, P. Ma and J. Lin, *Biomaterials*, 2014, **35**, 6359.
45 O. Terasaki, T. Ohsuna, Z. Liu, Y. Sakamoto and A. E. García-Bennet, *Stud. Surf. Sci. Catal.,* 2004, **148***,* 261.
46 M. Martínez-Carmona, M. Colilla, M. L. Ruiz-González, J. M. González-Calbet and Vallet-Regí, *Microporous Mesoporous Mater.,* 2016, **225**, 399.
47 B. González, M. Colilla, C. López de Laorden and M. Vallet-Regí, *J. Mater Chem.,* 2009, **19**, 9012.
48 A. J. Kuijpers, G. H. Engbers, J. Krijgsveld, S. A. Zaat, J. Dankert, and J. Feijen, *J. Biomater. Sci. Polym. Ed.,* 2000, , **11**, 225.
49 *T. Ito, L. Sun, M. A. Bevan and R. M. Crooks, Langmuir, 2004, **20**, 6940*
50 *T. Chen, W. Wu, H. Xiao, Y. Chen, M. Chen and J. Li, ACS Macro Lett., 2016, **5**, 55*
51 F. Balas, M. Manzano, M. Colilla and M. Vallet-Regí, *Acta Biomater.,* 2008, **4**, 514.
52 S. Young, M. Wong, Y. Tabata and A. G. Mikos, *J. Control. Release,* 2005, **109**, 256.
53 B. Gaihre, M.S. Khil, D. R. Lee and H. Y. Kim, *Int. J. Pharm.,* 2009, **365**, 180.
54 A. Martínez-Ruvalcaba, F. Becerra-Bracamontes, J. C. Sánchez-Díaz, A. González-Álvarez, *Polym. Bull.,* 2009, **62**, 539.
55 M. Vallet-Regí, M. Colilla and B. González, *Chem. Soc. Rev.* 2011, **40**, 596.
56 M. Wu, W. Gunning and M. Ratnam, *Cancer Epidemiol. Biomark. Prev.,* 1999, **8**, 775.
57 F. Shen, J. F. Ross, X. Wang and M. Ratnam, *Biochem.,* 1994, **33**, 1209.